Dislocation Networks and the Microstructural Origin of Strain Hardening

Ryan B. Sills,[1,2,*] Nicolas Bertin,[2] Amin Aghaei,[2] and Wei Cai[2,†]
[1]Sandia National Laboratories, Livermore, California 94551, USA
[2]Department of Mechanical Engineering, Stanford University, Stanford, California 94305, USA

(Received 3 April 2018; published 20 August 2018)

When metals plastically deform, the density of line defects called dislocations increases and the microstructure is continuously refined, leading to the strain hardening behavior. Using discrete dislocation dynamics simulations, we demonstrate the fundamental role of junction formation in connecting dislocation microstructure evolution and strain hardening in face-centered cubic (fcc) Cu. The dislocation network formed consists of line segments whose lengths closely follow an exponential distribution. This exponential distribution is a consequence of junction formation, which can be modeled as a one-dimensional Poisson process. According to the exponential distribution, two non-dimensional parameters control microstructure evolution, with the hardening rate dictated by the rate of stable junction formation. Among the types of junctions in fcc crystals, we find that glissile junctions make the dominant contribution to strain hardening.

DOI: 10.1103/PhysRevLett.121.085501

The flow stress required to continuously deform a crystal generally increases with the amount of plastic strain; this phenomenon is called strain hardening. The strain hardening rate is one of the most prominent features of the stress-strain curves of materials, and it is critical for the stability of plastic flow against local necking [1]. A quantitative understanding of the strain hardening rate in terms of fundamental physical mechanisms has attracted significant interest not only as a challenging problem in nonequilibrium statistical mechanics [2–8] but also for its importance in advanced manufacturing processes [9] (e.g., forming and cold working) and novel alloy design [10].

At temperatures below about one-third of the melting point of a metal, movement of dislocations—line defects in the crystal lattice—is the dominant mechanism for plastic deformation. It is widely believed that under such conditions, the strain hardening behavior of pure, single crystalline metals is entirely governed by the dynamics of dislocations, which multiply and form intricate network structures during plastic deformation. Through extensive theoretical and experimental research over the last five decades [11], a great deal is now known regarding the dislocation processes and strain hardening behaviors of single crystals. The mobility of individual dislocations and reactions between them are well understood through elasticity theory [7,12–16] and atomistic simulations [17–20]. Dislocation microstructures have been extensively characterized using transmission electron microscopy [21–23]. The stress-strain curves for single crystals have also been measured under a wide range of temperatures and loading directions [24]. However, a quantitative connection between the key microstructural features of the dislocation network and the strain hardening rate of a metal is still lacking.

In principle, the missing connection can be provided by large-scale discrete dislocation dynamics (DDD) simulations, which follow the evolution of the dislocation network and predict the stress-strain curve of the crystal. Using the ParaDiS program [25,26] and a recently developed time integrator [27], we can now predict the stress-strain curves of single crystal Cu along the [001] direction to a sufficient amount of strain so that the strain hardening rate can be obtained consistently. Our DDD simulations reveal an important microstructural feature of the dislocation network: the lengths of dislocation line segments (between junction nodes) closely obey an exponential distribution. This exponential distribution is parametrized by the dislocation density ρ, and a dimensionless parameter $\phi \equiv N^2/\rho^3$, where N is total number of the dislocation line segments per unit volume. We show that the exponential length distribution is the result of a one-dimensional Poisson process, where a dislocation line segment is randomly subdivided into two shorter segments when a stable junction is formed. Furthermore, junction formation is found to be essential for dislocation multiplication and strain hardening, because the strain hardening rate vanishes when junction formation is disabled in DDD simulations. Based on the exponential distribution of line lengths, a quantitative connection is established between the junction formation rate and the strain hardening rate, and, by selectively disabling different junction types in DDD simulations, we find that glissile junctions make the dominant contribution to the strain hardening rate.

Our DDD simulation cell is a cube with a 15 μm length subjected to periodic boundary conditions in all three

directions. The initial condition consists of straight dislocation lines on $\{111\}$ planes with $\frac{1}{2}\langle 011\rangle$ Burgers vectors. These dislocations are randomly chosen to have an edge, screw, or mixed (60°) character, and are confined to glide on $\{111\}$ planes (no cross-slip allowed). A linear mobility is applied to all mobile dislocations with a drag coefficient of $B = 15.6\ \mu$Pa s. The elastic interactions between dislocations are parametrized by the shear modulus $\mu = 54.6$ GPa and Poisson's ratio $\nu = 0.324$ of Cu. The dislocation structure is first relaxed to an equilibrium state, giving the initial density ρ_0, and it is then subjected to a constant strain rate $\dot{\varepsilon}$ along [001]. Under this high-symmetry loading condition, eight of the twelve slip systems have the same resolved shear stress with a Schmid factor $S \approx 0.41$, and the remaining four have a Schmid factor of zero.

Figure 1 shows the shear stress-strain curves predicted by DDD simulations under two strain rates, where the shear stress τ and strain γ are related to normal stress σ and strain ε by $\tau = S\sigma$ and $\gamma = \varepsilon/S$. Three independent simulations with randomly generated initial conditions are performed for each strain rate and initial density to insure robustness of the results—additional results with different initial densities are in the Supplemental Material (SM) [28].

As shown in Fig. 1, despite the fact that our strain rates are quite high relative to quasistatic experiments, the strain hardening rate is largely consistent with the Stage II hardening rate of $\Theta \equiv d\tau/d\gamma \sim 320 \pm 50$ MPa observed by Takeuchi [33] in single crystalline copper, and the commonly cited rules-of-thumb of $\mu/200$ to $\mu/300$ (180–270 MPa), where μ is the shear modulus, for fcc metals in Stage II [6,21]. The consistency in the slope of the stress-strain curves in Fig. 1 shows that the strain hardening rate is less sensitive to the applied strain rate than the yield stress.

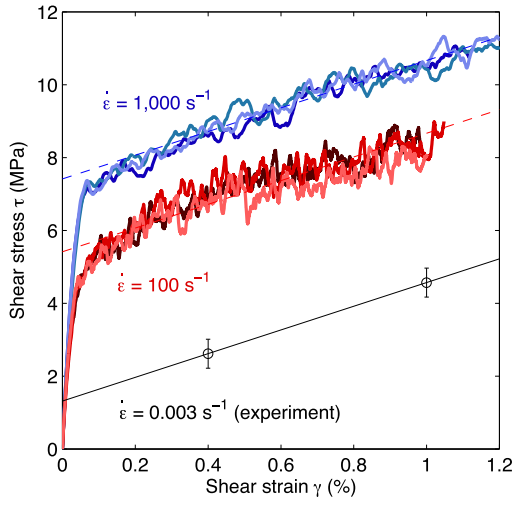

FIG. 1. Shear stress-strain curves of single crystalline Cu deformed along [001] axis. Thick curves are predictions by DDD simulations for an initial dislocation density $\rho_0 = 0.7 \times 10^{12}$ m^{-2} at two different strain rates $\dot{\varepsilon}$. The thin solid line is extracted from experimental data [33] at strain rate of $\dot{\varepsilon} = 3 \times 10^{-3}$ s^{-1}. The dashed lines are translated from the thin solid line to show the consistency of the strain hardening rate between simulations and experiments.

The success of DDD simulations in capturing the strain hardening rate of single crystals enables us to answer the fundamental question: which microstructural features in the dislocation network are responsible for the strain hardening behavior? An obvious candidate is the total dislocation density ρ. In fact, the well-known Taylor relation states that the flow stress τ satisfies the following relation,

$$\tau = \alpha\mu b\sqrt{\rho}, \tag{1}$$

where b is the magnitude of the Burgers vector, and α is a constant experimentally determined to be between 0.5 and 1 [5]. We find that the Taylor relation is obeyed during hardening in our DDD simulations with $\alpha \approx 0.5$ (see SM [28]).

The Taylor relation has often been interpreted by considering the critical stress needed to free (or activate) dislocations whose end points are pinned (e.g., by junctions) [34], by assuming that the average segment length scales with $\rho^{-1/2}$. Figure 2(a) shows a typical dislocation microstructure from our DDD simulations. The dislocation line network is quite complex and the segment lengths are clearly not all the same as is often assumed in simple models. Given the fundamental connection between dislocation line length and flow stress, the distribution of line lengths should be of primary importance when characterizing the statistical properties of dislocation networks, although in the past it has not received much attention. In this work, we have analyzed the length of all dislocation lines connecting one pinning point (e.g., nodes terminating at junctions) to another, which has been referred to as the link length [35]. We have performed such an analysis both on instantaneous snapshots from DDD simulations, as well as on configurations after the snapshots are relaxed under zero stress (similar to postmortem analysis in experiments).

Figure 2(b) shows the distribution of link lengths l normalized by the average length $\bar{l}$ from a typical relaxed dislocation structure at $\gamma = 0.87\%$ shear strain. The histogram shows that the probability distribution of link lengths can be well described by an exponential distribution,

$$p(l) = (1/\bar{l})e^{-l/\bar{l}}. \tag{2}$$

Other researchers have found that dislocation networks observed in molecular dynamics simulations of strained nanopillars exhibit a similar exponential distribution [36]. For the distribution shown in Fig. 2(b), we find that for link lengths less than $2.5\bar{l}$ (which comprises 91% of the links), the deviation from the exponential distribution in a quantile-quantile (Q-Q) plot is less than 5% (see SM [28]).

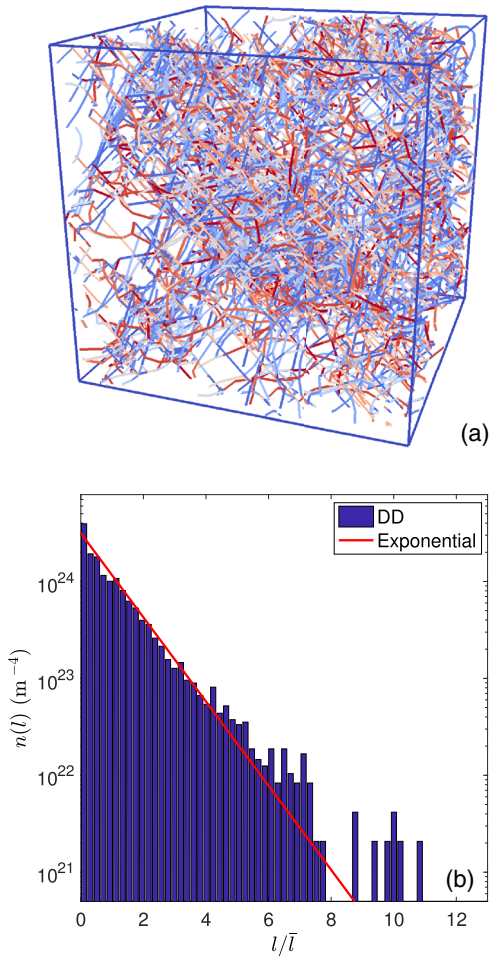

FIG. 2. (a) Snapshot from a DDD simulation at $\gamma = 0.87\%$ shear strain, with $\dot{\varepsilon} = 10^3$ s^{-1} and $\rho_0 = 0.7 \times 10^{12}$ m^{-2}. (b) Dislocation link length distribution $n(L)$ for the structure shown in (a) (after being relaxed to zero stress) compared to Eq. (3).

To discuss the nature of the exponential length distribution and its consequence on strain hardening, it is useful to introduce a length density function, $n(l) \equiv Np(l)$, where $n(l)dl$ is the number of links per unit volume whose length is between l and $l + dl$. N is the total number of links per unit volume. N and ρ are the zeroth and first moments of the density function $n(l)$, respectively. If we define a nondimensional parameter $\phi \equiv N^2/\rho^3$, then the average link length is $\bar{l} = \rho/N = 1/\sqrt{\phi\rho}$, and Eq. (2) is equivalent to

$$n(l) = \phi\rho^2 e^{-\sqrt{\phi\rho}l}. \tag{3}$$

Equation (3) means that the dislocation length distribution is completely determined by the total density ρ and the nondimensional parameter ϕ. We find that ϕ gradually increases during the course of the simulations (see Fig. 3).

The exponential form of $n(l)$ can be explained by considering a simple model for the junction formation process. The degrees of freedom of the model are the

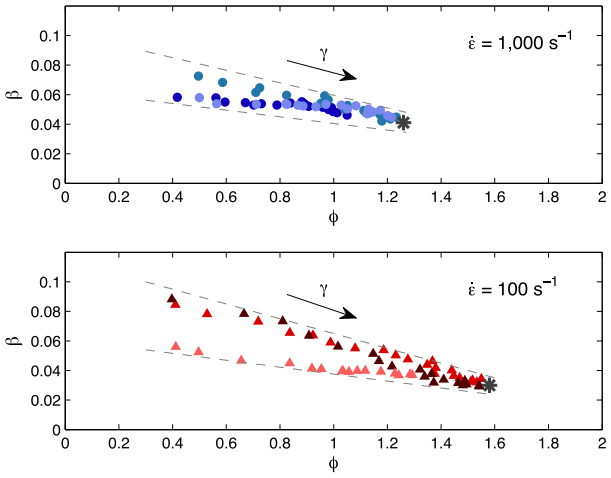

FIG. 3. $\phi - \beta$ values during DDD simulations at strain rates $\dot{\varepsilon} = 10^3$ s^{-1} and 10^2 s^{-1}. Dashed lines are guide to the eye for the range of $\phi - \beta$ values. The * symbol indicates the critical value ϕ_c, beyond which Eq. (7) becomes valid.

lengths l of N dislocation links in a unit volume. When a link of length l participates in a junction formation event, we assume that this link splits into two links of lengths l_1 and $l_2 = l - l_1$, where l_1 is uniformly distributed in $(0, l)$. If we assume that the probability rate for splitting a link is proportional to its length l, then numerical simulations show that the distribution of link lengths quickly goes to an exponential distribution (see SM [28]). Therefore, we attribute the origin of the link length distribution to the observation that the probability of a link of length l experiencing a collision is proportional to l, rendering junction formation a one-dimensional Poisson point process from which an exponential distribution results [37]. In other words, the probability of finding a link of length l having not yet suffered a collision is exponentially small ($\sim e^{-l/\bar{l}}$).

In the following, we show that focusing on the dislocation link length distribution function, $n(l)$, allows us to reveal deeper connections between the dislocation microstructure and the strain hardening rate that have not been appreciated before. We shall assume that $n(l)$ (in single crystal Cu under [001] loading) always follows the exponential distribution of Eq. (3), which is parametrized by the dislocation density ρ and a nondimensional parameter ϕ. Furthermore, we shall assume that the dislocation microstructure (under [001] loading) is uniquely determined by the two parameters ρ and ϕ. Given these assumptions, we will be able to establish a quantitative link between the junction formation rate and the strain hardening rate, as shown below.

Consistent with the assumption that the probability rate of a line splitting is proportional to its length l, we assume that the overall collision rate between dislocations on different slip systems is $R = f\rho^2\bar{v}$, where f is the ratio of the forest density ρ_f over the total density ρ, and the

mean spacing between pinning points on dislocation slip planes is $\lambda \equiv 1/\sqrt{f\rho}$. Our DDD simulations show that $f \approx 0.45$ and remains a constant with strain (see SM [28]). The difference between ϕ (increasing with strain) and f (constant) means that the average link length $\bar{l}$ is different from λ. $\bar{v}$ is the average dislocation velocity related to the strain rate $\dot{\gamma}$ through the Orowan equation, $\dot{\gamma} = \rho b \bar{v}$. Since not all collisions result in the formation of a stable junction, we introduce a nondimensional parameter β, which is the fraction of collisions that leads to stable junction formation, so that the junction formation rate is βR. We assume that each time a stable junction forms, two dislocation links become four links, so that the rate at which the number of links increases is

$$\dot{N} = 2\beta f \rho^2 \bar{v} = \frac{2\beta f \rho}{b}\dot{\gamma}. \tag{4}$$

Assuming that the exponential distribution is always maintained, it follows that $N = \phi^{1/2}\rho^{3/2}$ and $\dot{N} = \frac{3}{2}\phi^{1/2}\rho^{1/2}\dot{\rho} + \frac{1}{2}\phi^{-1/2}\rho^{3/2}\dot{\phi}$, leading to the dislocation multiplication rate

$$\dot{\rho} = \frac{4\beta f \dot{\gamma}}{3\sqrt{\phi} b}\sqrt{\rho} - \frac{\dot{\phi}}{3\phi}\rho. \tag{5}$$

Interestingly, the dislocation multiplication rate expression in Eq. (5) is consistent with the Kocks-Mecking model [6], $\dot{\rho} = K_1\sqrt{\rho} - K_2\rho$, with $K_1 = [(4\beta f\dot{\gamma})/(3\sqrt{\phi}b)]$ and $K_2 = [\dot{\phi}/(3\phi)]$. Here, we see that the Kocks-Mecking form appears as a natural consequence of the exponential distribution of link lengths, although the physical origin and temperature dependence of Eq. (5) is different from the original Kocks-Mecking model. Combining Eq. (5) with the Taylor relation, Eq. (1), the strain hardening rate is,

$$\Theta = \frac{\dot{\tau}}{\dot{\gamma}} = \frac{1}{3}\alpha\mu\left(\frac{2\beta f}{\sqrt{\phi}} - \frac{b\sqrt{\rho}}{2\phi}\frac{\dot{\phi}}{\dot{\gamma}}\right). \tag{6}$$

Equation (6) shows that the strain hardening rate Θ is determined by the junction formation rate β, as well as $\dot{\phi}/\dot{\gamma}$, the rate at which parameter ϕ changes with strain γ.

We can analyze the different contributions to the strain hardening rate Θ in our DDD simulations in light of Eq. (6). Specifically, we compute the dislocation density ρ and link number density N from a series of DDD simulation snapshots, and extract the nondimensional parameters ϕ and β using $\phi = N^2/\rho^3$ and $\beta = b\dot{N}/(2f\rho\dot{\gamma})$. Given the assumption that the dislocation microstructure always obeys the exponential distribution Eq. (3) (for Cu in [001] loading), which is completely governed by parameters ρ and ϕ, we expect that all properties of the network should be functions of ρ and ϕ. The junction formation rate β is just a property of the dislocation network, and it should therefore be a function of ρ and ϕ. Hence, for simulations starting from the same initial dislocation density ρ_0 and at the same strain rate $\dot{\gamma}$, we expect β (on average) to be a function of ϕ.

Figure 3 shows the evolution of dislocation microstructure in the nondimensional space of $\beta - \phi$. It is observed that during the course of the simulation, ϕ gradually increases from about 0.4 to as high as about 1.6, accompanied by a decrease in β. This indicates that during this early period of strain hardening, the dislocation microstructure does not evolve in a self-similar manner—not only does the density ρ increase, but the nondimensional parameter ϕ also increases. However, the rate of increase of ϕ slows down with increasing strain, so that if ϕ exceeds a critical value ϕ_c, which occurs at $\gamma \approx 1\%$, $\dot{\phi}/\dot{\gamma}$ becomes so small that the second term in Eq. (6) becomes negligible compared to the first term (see SM [28]). In this case, the strain hardening rate can be approximated as

$$\Theta \approx \frac{2\alpha\beta f}{3\sqrt{\phi}}\mu. \qquad (\phi \geq \phi_c). \tag{7}$$

Equations (6) and (7) motivate the hypothesis that the net junction formation fraction β is the controlling factor of the dislocation multiplication rate and strain hardening rate. In other words, if the dislocations were not allowed to form more junctions, the network would not have the capacity to store more dislocations and there would not be any strain hardening. In order to test this hypothesis, we employed specialized DDD simulations in which junction formation events are suppressed. With our approach (see SM [28]), we are able to suppress selected types of junctions, enabling us to assess the role of each junction type (collinear, glissile, Hirth, and Lomer [38,39]). This illustrates the power of computational tools such as DDD in answering fundamental questions by examining scenarios not accessible by experiments.

Figure 4 shows the stress-strain curves obtained with these specialized simulations. When all junctions are suppressed, the hardening rate (at $\dot{\varepsilon} = 10^3\ \mathrm{s}^{-1}$) is greatly reduced from 329 to 47 MPa. We believe the strain hardening rate does not completely vanish in this case because our modifications do not completely eliminate junction formation events. When only one type of junction is allowed to form, the hardening rate is approximately 225, 117, 103, and 46 MPa for glissile, collinear, Lomer, and Hirth junctions, respectively. This result indicates that glissile junctions make the dominant contribution to strain hardening. This finding is interesting because the collinear junction is the strongest among the four junctions [14]. We believe that glissile junctions make the largest contribution because they are relatively stable [15] and are the most likely to form, with four forest interactions per slip system (compared to two, two, and one for Lomer, Hirth, and collinear, respectively; see SM [28] for further elaboration).

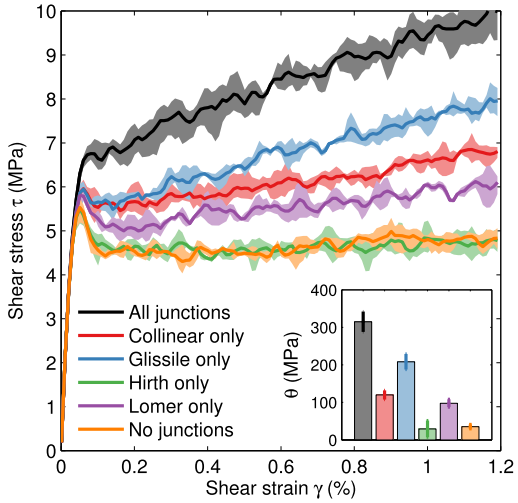

FIG. 4. Shear stress-strain curves and (inset) strain hardening rates for specialized DDD simulations with selected types of junctions suppressed; $\rho_0 = 0.7 \times 10^{12}$ m^{-2} and $\dot{\varepsilon} = 10^3$ s^{-1}. The legend shows the type of junctions that are allowed to form during the simulation.

Our DDD simulations have shown that the dislocation link lengths satisfy an exponential distribution, that junction formation is a necessity for strain hardening, and that glissile junctions make the dominant contribution to the strain hardening rate in [001] loading of Cu. The exponential distribution is explained by a simple model for the effect of junction formation on the population of dislocation lines. Analysis using the exponential length distribution reveals a fundamental connection between the junction formation rate (β) and the strain hardening rate (Θ). We hope this work brings attention to the dislocation link length distribution as an important property of the dislocation microstructure, so that it may be incorporated in future coarse-grained field theories of dislocation dynamics and dislocation-based crystal plasticity models.

This work was supported by Sandia National Laboratories (R. B. S.) and by the U.S. Department of Energy, Office of Basic Energy Sciences, Division of Materials Sciences and Engineering under Award No. DE-SC0010412 (N. B., A. A. and W. C.). Sandia National Laboratories is a multimission laboratory managed and operated by National Technology and Engineering Solutions of Sandia, LLC, a wholly owned subsidiary of Honeywell International, Inc., for the U.S. Department of Energy's National Nuclear Security Administration under Contract No. DE-NA0003525. This paper describes objective technical results and analysis. Any subjective views or opinions that might be expressed in the paper do not necessarily represent the views of the U.S. Department of Energy or the United States Government.

*Corresponding author.
rbsills@sandia.gov
†caiwei@stanford.edu

[1] A. K. Ghosh, Acta Metall. **25**, 1413 (1977).
[2] J. Friedel, Philos. Mag. **46**, 1169 (1955).
[3] A. Seeger, J. Diehl, S. Mader, and H. Rebstock, Philos. Mag. **2**, 323 (1957).
[4] F. R. N. Nabarro, Z. S. Basinski, and D. B. Holt, Adv. Phys. **13**, 193 (1964).
[5] H. Mecking and U. F. Kocks, Acta Metall. **29**, 1865 (1981).
[6] U. F. Kocks and H. Mecking, Prog. Mater. Sci. **48**, 171 (2003).
[7] V. V. Bulatov, L. L. Hsiung, M. Tang, A. Arsenlis, M. C. Bartelt, W. Cai, J. N. Florando, M. Hiratani, M. Rhee, G. Hommes, T. G. Pierce, and T. D. de la Rubia, Nature (London) **440**, 1174 (2006).
[8] B. Devincre, T. Hoc, and L. Kubin, Science **320**, 1745 (2008).
[9] *Metal Forming: Mechanics and Metallurgy*, edited by W. F. Hosford and R. M. Caddell (Cambridge University Press, New York, 2011).
[10] *Alloy and Microstructural Design*, edited by J. K. Tien and G. S. Ansell (Academic Press, New York, 1976).
[11] P. M. Anderson, J. P. Hirth, and J. Lothe, *Theory of Dislocations*, 3rd ed. (Cambridge University Press, 2017).
[12] V. B. Shenoy, R. V. Kukta, and R. Phillips, Phys. Rev. Lett. **84**, 1491 (2000).
[13] R. Madec, B. Devincre, and L. P. Kubin, Phys. Rev. Lett. **89**, 255508 (2002).
[14] R. Madec, B. Devincre, L. Kubin, T. Hoc, and D. Rodney, Science **301**, 1879 (2003).
[15] L. P. Kubin, R. Madec, and B. Devincre, in *MRS Symposium Proceedings*, edited by H. Zbib, D. Lassila, L. Levine, and K. Hemker (Materials Research Society, Warrendale, 2003), Vol. 779, pp. 25–26.
[16] B. Devincre, L. Kubin, and T. Hoc, Scr. Mater. **54**, 741 (2006).
[17] D. Rodney and R. Phillips, Phys. Rev. Lett. **82**, 1704 (1999).
[18] V. V. Bulatov and W. Cai, Phys. Rev. Lett. **89**, 115501 (2002).
[19] D. L. Olmsted, L. G. Hector, W. A. Curtin, and R. J. Clifton, Model. Simul. Mater. Sci. Eng. **13**, 371 (2005).
[20] C. R. Weinberger and W. Cai, Scr. Mater. **64**, 529 (2011).
[21] S. J. Basinski and Z. S. Basinski, in *Dislocations in Solids*, edited by F. Nabarro (North-Holland Publishing Company, Amsterdam, 1979), Chap. 16, pp. 261–362.
[22] N. Hansen and D. A. Hughes, Phys. Status Solidi A **149**, 155 (1995).
[23] C. Hong, X. Huang, and G. Winther, Philos. Mag. **93**, 3118 (2013).
[24] R. W. K. Honeycombe, *The Plastic Deformation of Metals* (Edward Arnold, London, 1984).
[25] A. Arsenlis, W. Cai, M. Tang, M. Rhee, T. Oppelstrup, G. Hommes, T. G. Pierce, and V. V. Bulatov, Model. Simul. Mater. Sci. Eng. **15**, 553 (2007).
[26] "Parallel Dislocation Simulator (ParaDiS)", http://paradis.stanford.edu.
[27] R. B. Sills, A. Aghaei, and W. Cai, Model. Simul. Mater. Sci. Eng. **24**, 045019 (2016).

[28] See Supplemental Material at http://link.aps.org/supplemental/10.1103/PhysRevLett.121.085501 for additional results and analysis, which includes Refs. [29–32].
[29] W. Cai, A. Arsenlis, C. R. Weinberger, and V. V. Bulatov, J. Mech. Phys. Solids **54**, 561 (2006).
[30] P. Hähner, K. Bay, and M. Zaiser, Phys. Rev. Lett. **81**, 2470 (1998).
[31] M. Zaiser, K. Bay, and P. Hähner, Acta Mater. **47**, 2463 (1999).
[32] J. G. Sevillano, E. Bouchaud, and L. P. Kubin, Scr. Metall. Mater. **25**, 355 (1991).
[33] T. Takeuchi, Trans. Jpn. Inst. Met. **16**, 629 (1975).
[34] G. Saada, Acta Metall. **8**, 841 (1960).
[35] R. Lagneborg and B. H. Forsen, Acta Metall. **21**, 781 (1973).
[36] G. Z. Voyiadjis and M. Maghoobi, Scr. Mater. **130**, 182 (2017).
[37] N. Lanchier, *Stochastic Modeling* (Springer, Switzerland, 2017).
[38] J. P. Hirth, J. Appl. Phys. **32**, 700 (1961).
[39] L. P. Kubin, *Dislocations, Mesoscale Simulations, and Plastic Flow* (Oxford University Press, Oxford, UK, 2013).